Axial stress–strain relationship for FRP confined circular and rectangular concrete columns

Mohamed H. Harajli *

Department of Civil and Environmental Engineering, American University of Beirut, Beirut-Lebanon, Lebanon

Available online 30 August 2006

Abstract

A general mathematical model is developed to describe the stress–strain (f_c–ε_c) relationship of FRP confined concrete. The relationship is applicable to both circular and rectangular columns, and accounts for the main parameters that influence the stress–strain response. These include the area and material properties of the external FRP wraps, the aspect ratio of rectangular column sections, the corner radius used for FRP application, and the volumetric ratio and configuration of internal transverse steel. The proposed model reproduced accurately experimental results of stress–strain or load–deformation response of circular and rectangular columns. In addition to its importance in evaluating the effect of FRP confinement on the ultimate axial strength of concrete columns, the developed f_c–ε_c relationship can be employed very efficiently and effectively for analyzing the response of FRP confined concrete under different types of load application.
© 2006 Elsevier Ltd. All rights reserved.

Keywords: Columns; Confined concrete; Ductility; Fiber reinforced polymers; Stress; Strain

1. Introduction

Several experimental studies have been conducted for evaluating the axial strength characteristics of concrete columns confined externally with fiber reinforced polymer (FRP) composites. These studies have identified most of the critical parameters that influence the axial strength of FRP confined columns [1]. These include the area and material properties of the transverse FRP reinforcement, arrangement of reinforcement, type of column section (rectangular, circular), the aspect ratio of rectangular section, and the radius of the section corner prepared for FRP application. Although most of these parameters are identical to those that influence the stress–strain response of steel confined concrete, because steel behaves in elasto-plastic manner while FRP is a linear elastic material, the axial strength and stress–strain behavior for concrete confined with FRP composites are substantially different as compared to concrete confined with steel ties.

Most of the available studies on the axial strength characteristics of FRP confined columns have concentrated on circular columns, while relatively very few addressed rectangular columns [2,3]. Similar to the behavior of steel confined concrete [4], lateral confinement of rectangular sections using FRP, particularly those with large aspect ratio, is not as effective as circular sections [5]. Unlike circular columns where the full column section is confined, rectangular columns need sizable axial strain before the flat sides are able to mobilize the FRP confinement pressure. According to ACI Committee 440 [1], confining square or rectangular columns with FRP jackets can provide marginal increase in the axial load capacity, but because of the many unknowns associated with this type of application, it is not possible with the current state of knowledge to provide recommendations on the use of FRP for strengthening rectangular columns. Furthermore, because of the substantial number of parameters involved, very

---

* Tel.: +961 3 627180; fax: +961 1 744462.
  E-mail address: mharajli@aub.edu.lb

Nomenclature

A_{frp}	area of transverse FRP reinforcement	n_f	number of transverse FRP layers
A_{fa}	area of longitudinal FRP reinforcement	P	applied axial load
A_g	gross area of section	r	corner radius
A_{cc}	area of concrete core	s'	clear spacing between transverse hoops or spirals
A_e	area of effectively confined concrete		
A_s	area of column longitudinal reinforcement	t_f	thickness of one FRP layer
b	section width	w	clear distance between adjacent longitudinal bars
D	diameter of circular section		
d_s	diameter of spiral or hoop	w_{xi}, w_{yi}	the ith clear distance between adjacent longitudinal bars along the horizontal x- and y-dimensions respectively
E_c	modulus of elasticity of concrete		
E_f	modulus of elasticity of transverse FRP		
E_{fa}	modulus of elasticity of longitudinal FRP	x, y	concrete core dimensions to center line of peripheral hoop
E_{lf}	lateral modulus of elasticity of FRP		
E_{ls}	lateral modulus of elasticity of steel	ε_c	concrete strain
E_s	modulus of elasticity of steel	ε_{cc}	concrete strain for confined concrete
f_c	concrete stress	ε_{co}	concrete strain at the intersection point between the 1st and 2nd stage of the stress–strain curve
f'_c	compressive strength of unconfined concrete		
f_{cc}	stress in confined concrete	ε_{cu}	limiting concrete strain
f'_{cc}	compression strength of confined concrete	ε_{fu}	fracture strain of the FRP
f_{co}	stress at the intersection point between the 1st and 2nd stage of the stress–strain curve	ε_ℓ	lateral concrete strain
		$\varepsilon_{\ell o}$	lateral concrete strain at intersection point between the 1st and 2nd stage of the stress–strain curve
f_{cu}	stress corresponding to a limiting strain ε_{cu}		
f_ℓ	effective lateral confining pressure	ε_o	strain at maximum stress for unconfined concrete
f'_ℓ	hydrostatic confining pressure		
f_s	steel stress	ε_{yt}	yield strain of transverse hoops
f_y	yield stress of longitudinal column reinforcement	ρ_{cc}	steel ratio relative to the concrete core section
f_{yt}	yield stress of transverse steel ties or hoops	ρ_f	volumetric ratio of FRP reinforcement
h	section depth	ρ_s	ratio of column longitudinal reinforcement
k_1	confinement effectiveness coefficient	ρ_{st}	volumetric ratio of hoop reinforcement
k_e, k_v	confinement effectiveness parameters		

few studies have attempted to generate the stress–strain response of concrete confined with FRP composites taking into account rectangular sections. In evaluating the axial–flexural capacity of concrete columns confined with FRP straps, Saadatmanesh et al. [6] adopted the stress–strain model of Mander at al. [4] which was developed for concrete confined with ordinary steel. However, as pointed out by Mirmiran and Shahawy [7], given the significantly different mechanical properties of the steel and FRP, extending confinement models developed originally for steel to cover FRP confined columns may not be appropriate. A stress–strain model for FRP confined concrete was developed by Toutanji [8] but it is applicable mainly for circular columns.

In this study, a comprehensive and yet simple mathematical model is developed to produce the stress–strain response of FRP confined concrete column sections. In addition to its great importance in predicting the effect of FRP confinement on the axial load capacity of columns, the generation of such a stress–strain relationship is essential for conducting analytical studies of the response of

FRP confined concrete under different types of load applications, including axial and flexural loads [9].

2. Confinement models

Most of the available models for evaluating the compression strength and ductility of confined concrete are based on the confinement model derived experimentally by Richart et al. [10,11] using concrete specimens confined with active hydrostatic fluid pressure

$$f'_{cc} = f'_c + k_1 f'_\ell \tag{1a}$$

$$\varepsilon_{cc} = \varepsilon_o \left(1 + k_2 \frac{f'_\ell}{f'_c} \right) \tag{1b}$$

where f'_{cc}, ε_{cc} are the compressive strength and corresponding strain of confined concrete; f'_c, ε_o are the compressive strength and corresponding strain for unconfined concrete; f'_ℓ is the lateral hydrostatic pressure; $k_1 = 4.1$, and $k_2 = 5k_1$.

Among the most widely used models to describe the axial strength of reinforced concrete columns confined with

transverse steel is the one proposed by Mander et al. [4] based on the work of Elwi and Murray [12], in which the confined concrete compressive strength f'_{cc} and corresponding strain ε_{cc} are expressed as a function of the effective lateral confining pressure f_ℓ as follows:

$$f'_{cc} = f'_c \left(-1.254 + 2.254 \sqrt{1 + \frac{7.94 f_\ell}{f'_c}} - 2\frac{f_\ell}{f'_c} \right) \qquad (2a)$$

$$\varepsilon_{cc} = \varepsilon_o \left[1 + 5 \left(\frac{f'_{cc}}{f'_c} - 1 \right) \right] \qquad (2b)$$

Numerous experimentally and analytically derived strength models were developed to calculate the confinement effectiveness coefficient k_1 for FRP confined concrete. These models either adopt Eq. (2a) by Mander et al. without modification (ACI Committee 440 [1]) or with slight calibration to fit experimental data, or express k_1 as a constant or as a function of the effective lateral confining pressure f_ℓ. A summary and evaluation of existing strength models for steel confined concrete or concrete confined externally with FRP composites were reported by Mirmiran and Shahawy [7] and more recently by Teng and Lam [13,14].

In evaluating the stress–strain behavior of FRP confined concrete columns, Toutanji [8] used the following expression for the confinement effectiveness coefficient:

$$k_1 = 3.5 \left(\frac{f_\ell}{f'_c} \right)^{-0.15} \qquad (3)$$

Based on a statistical analysis of an extensive number of experimental data of circular unreinforced concrete column specimens, Lam and Teng [13] found that as most of the existing tests on FRP confined concrete show an approximately linear relationship between the strength of confined concrete and the lateral pressure, the additional complexity in representing this relationship in many of the existing models may be unwarranted. Based on this observation they proposed a constant value for $k_1 = 2.15$, which produced the closest predictions of the experimental data surveyed. However, in a more recent experimental study of FRP elliptical and circular columns, Teng and Lam [15] found that an average value of k_1 of 3.71 correlates better with their test data than a value of 2.15.

In this study, in addition to the great mathematical simplification that it offers in generating the stress–strain response, the use of a constant value of $k_1 = 4.1$ as initially proposed by Richart et al. [10,11] was found to produce the least discrepancy between the analytical predictions and experimental data. Note that within the practical range of confinement ratios where most of the available experimental data concentrates (f_ℓ/f'_c less than about 0.75), except for the conservative values given by Lam and Teng [13], the range of values of the confinement effectiveness f'_{cc}/f'_c predicted using either of Eq. (1a) corresponding to $k_1 = 4.1$, Eq. (2a), or Eq. (3) tends to be approximately similar (Fig. 1).
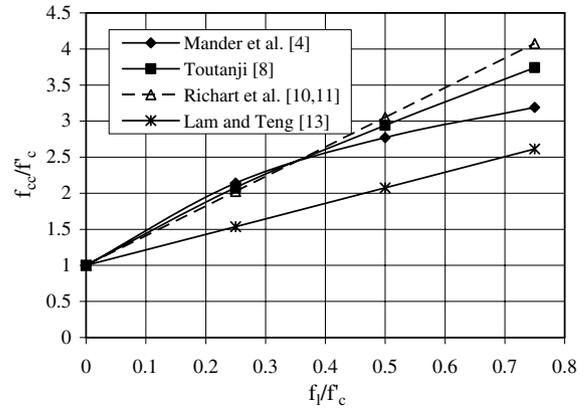

Fig. 1. Variation of confinement effectiveness with confinement ratio.

3. Constitutive stress–strain relationship

In this study, a two-stage relationship of the stress–strain (f_c–ε_c) response for FRP confined concrete is derived. The corresponding relationship is shown schematically in Fig. 2 in comparison with typical stress–strain responses for unconfined concrete and concrete confined with transverse steel. Using analogy with steel confined concrete at low lateral or axial concrete strains before steel yielding, the stress–strain response of FRP confined concrete in the first stage can be described using a second degree parabola similar to that proposed by Scott et al. [16] for generating the ascending branch of the stress–strain relationship for unconfined concrete or concrete confined with transverse steel ties

$$f_c = f_{co} \left[\frac{2\varepsilon_c}{\varepsilon_{co}} - \left(\frac{\varepsilon_c}{\varepsilon_{co}} \right)^2 \right] \quad \text{for } \varepsilon_c \leqslant \varepsilon_{co} \qquad (4)$$

in which f_{co} and ε_{co} are the stress and strain at the intersection point between the first stage and the second stage. The
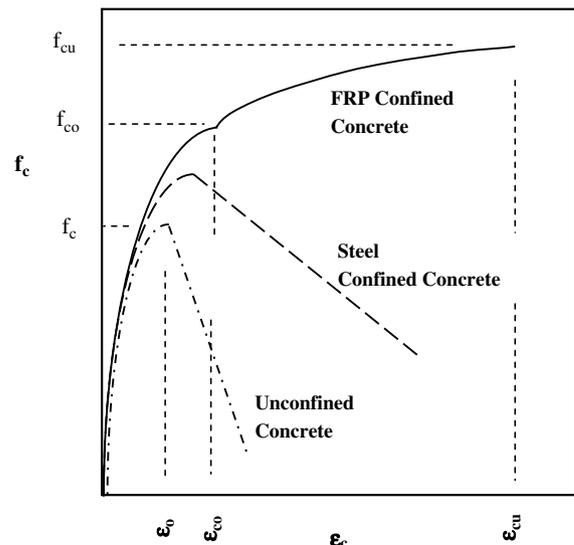

Fig. 2. Proposed stress–strain relationship for FRP confined concrete.

f_c–ε_c relationship in the second stage, including the intersection point f_{co}, depends on the relationship between the concrete lateral strain and axial strain; the confinement coefficient k_1 discussed earlier; the geometry of the section (circular, rectangular); the aspect ratio and corner radius for rectangular sections; the area and modulus of elasticity of the FRP material; and the area, configuration, and yield strength of internal transverse confining steel whenever available.

The relation between the lateral and axial concrete strain in the second stage of the stress–strain response, including the intersection point, is assumed to follow the expression used by Toutanji [8]:

$$\varepsilon_c = \varepsilon_o\left[1 + (310.57\varepsilon_\ell + 1.9)\left(\frac{f_c}{f_c'} - 1\right)\right] \quad (5)$$

in which ε_o is the axial strain at the peak concrete compressive stress for plain unconfined concrete, taken equal to 0.002. Note that Eq. (5) is similar in form to Eq. (2b) except that the confinement coefficient k_2 in Eq. (5) varies as a function of the lateral strain.

Using the concept of Eq. (1a), the axial stress of concrete confined with a combination of external FRP wraps and internal transverse ties, neglecting for simplicity the reduction in the concrete area due to longitudinal steel, can be expressed for the second stage of the stress–strain relationship, including the intersection point between the first and second stages ($f_c = f_{co}$), as

$$f_c = f_c' + k_1 f_{\ell f} + k_1 f_{\ell s}\frac{A_{cc}}{A_g} \quad (6)$$

where $k_1 = 4.1$, A_{cc} is the area of the concrete core confined with internal transverse ties, measured to outside perimeter of ties, and A_g is the gross area of the column section. The terms $f_{\ell f}$ and $f_{\ell s}$ are the lateral passive confining pressure exerted by FRP and ordinary transverse steel on the concrete section, respectively

$$f_{\ell f} = \left(\frac{k_{ef}\rho_f E_f}{2}\right)\varepsilon_\ell \quad (7)$$

$$f_{\ell s} = \left(\frac{k_{es}k_v\rho_{st}E_s}{2}\right)\varepsilon_\ell \leqslant \left(\frac{k_{es}k_v\rho_{st}}{2}\right)f_{yt} \quad (8)$$

The term ρ_f is the volumetric ratio of the FRP sheets. For a circular concrete section with diameter D, $\rho_f = 4n_f t_f/D$, while for a rectangular section with dimensions b and h (see Fig. 3), $\rho_f = 2n_f t_f(b + h)/bh$, where n_f is the number of transverse FRP applications (layers) and t_f is the design thickness of the FRP fabric; ρ_{st} is the volumetric ratio of the transverse steel ties or hoops (volume of ties or hoops to volume of concrete core measured to outside of hoops, neglecting the influence of cross ties); E_s is the modulus of elasticity of steel and f_{yt} is the yield strength of the transverse ties. The term $k_e(k_{ef}, k_{es}) = A_e/A_{cc}$, where A_e is the effective confined concrete area, accounts for the effectiveness of lateral confinement in confining the concrete in the horizontal plane; while the term k_v is a coefficient that accounts for the effectiveness of lateral confinement in confining the concrete along the longitudinal direction between the transverse hoops ($k_v = 1.0$ for concrete confined with continuous FRP sheets). For circular sections, the effectively confined concrete area is equal to the confined area A_{cc} and hence $k_{ef} = k_{es} = 1.0$. On the other hand, because the sides of rectangular hoops or FRP sheets in rectangular columns have the tendency to bend outward, the confinement pressure is transmitted to the section mainly through the corners. In this case the effectively confined concrete area could be significantly less than the area of the confined concrete core depending on the aspect ratio of the column section, configuration of internal transverse hoops, or the radius r of the section corners prepared for FRP application. Note that rounding the corners for FRP application in rectangular or sharp-edge sections is particularly important for preventing stress concentration and possible premature fracture of the FRP. ACI Committee 440.2R [1] recommends a minimum radius of 13 mm when wrapping FRP sheets around outside corners.

The effectively confined concrete area A_e can be estimated using the approach suggested by Sheikh and Uzumeri [17]. In this approach A_e is obtained by subtracting from the confined area the area of parabolas assumed to constitute the ineffectively confined concrete between longitudinal reinforcing bars or corners of FRP (see Fig. 3). The area of one parabola is equal to $(w)^2/6$ where w, for the case of concrete confined with internal hoops, is equal to the clear distance between adjacent longitudinal
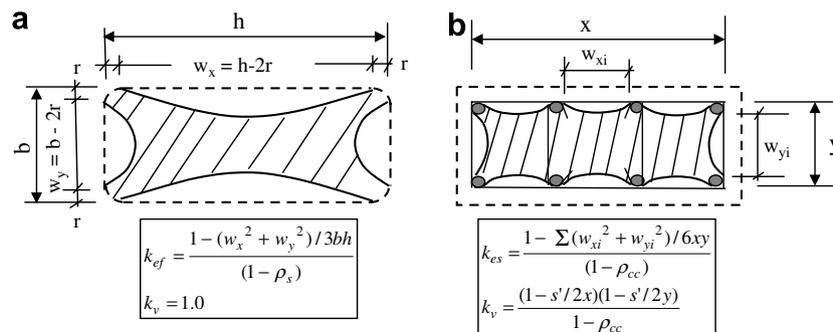

Fig. 3. Confinement effectiveness coefficients: (a) using FRP, (b) using hoops.

bars. The parameters k_{ef}, k_{es}, and k_v are expressed in Fig. 3 for rectangular columns based on the approach proposed by Sheikh and Uzumeri [17] and more recently by Mander et al. [4]. In Fig. 3 the term w_{xi} and w_{yi} are the ith clear distance between adjacent longitudinal bars along the horizontal x- and y-dimensions, respectively; x and y are the concrete core dimensions to center line of peripheral hoop; ρ_s and ρ_{cc} correspond to the longitudinal steel ratio for the whole section and the steel ratio relative to the confined concrete core measured to outside of hoops; and s' is the clear vertical spacing between the lateral hoops. For circular sections, k_v can be calculated using the following expressions [4]:

For concrete confined with circular hoops

$$k_v = \frac{\left(1 - \frac{s'}{2d_s}\right)^2}{1 - \rho_{cc}} \tag{9}$$

For concrete confined with spirals

$$k_v = \frac{1 - \frac{s'}{2d_s}}{1 - \rho_{cc}} \tag{10}$$

where d_s is the diameter of spiral or hoop.

In developing a two-stage relationship of the stress–strain behavior of FRP confined concrete, Toutanji [8] assumed that the intersection point between the first and second stages occurs at a lateral strain of 0.002. Note that for steel confined concrete, a lateral strain of 0.002 coincides with the strain at which the lateral steel yields, producing a change in the stress–strain response. The adoption of a somewhat similar assumption in the current investigation does not only lead to a significant simplification of the analytical model when accounting for the effect of internal steel confinement but also has the advantage of producing a consistent mathematical stress–strain model that remains valid at the boundaries between concrete confined only with FRP or concrete confined purely by transverse steel. Using this assumption, the stress f_{co} and strain ε_{co} for use with the first stage of the stress–strain relationship (Eq. (4)) can be calculated using Eqs. (6) and (5) as follows:

$$f_{co} = f'_c + k_1 \varepsilon_{\ell o} \left(\frac{k_{ef}\rho_f E_f}{2} + \frac{k_{es}k_v \rho_{st} E_s}{2}\left(\frac{A_{cc}}{A_g}\right)\right) \tag{11}$$

$$\varepsilon_{co} = \varepsilon_o \left[1 + (310.57\varepsilon_{\ell o} + 1.9)\left(\frac{f_{co}}{f'_c} - 1\right)\right] \tag{12}$$

where $\varepsilon_{\ell o}$ is taken equal to the yield strain ε_{yt} of transverse steel hoops or 0.002 if no internal confinement by transverse steel is available.

Beyond a lateral strain of $\varepsilon_{\ell o}$, or axial strain of ε_{co} calculated from Eq. (12), the f_c–ε_c relationship in the second stage of the response can be obtained by solving Eq. (5) for ε_ℓ and using it for the second term on the right-hand side of Eq. (6). The transverse steel is assumed to provide a constant lateral confining pressure $f_{\ell s} = \left(\frac{k_{es}k_v \rho_{st} E_s}{2}\right)\varepsilon_{\ell o}$ (see Eq. (8)), leading to the following comprehensive relationship:

$$f_c = \sqrt{(K_o^2 - K)} - K_o \tag{13a}$$

$$K_o = 0.0031 k_1 E_{lf} - f'_c - \frac{1}{2}k_1 E_{ls}\varepsilon_{\ell o}\frac{A_{cc}}{A_g} \tag{13b}$$

$$K = f'^2_c + k_1 f'_c E_{ls}\varepsilon_{\ell o}\frac{A_{cc}}{A_g} - 0.0032 k_1 E_{lf} f'_c\left(\frac{\varepsilon_c}{\varepsilon_o} + 0.9\right) \tag{13c}$$

where

$$E_{lf} = k_{ef}\rho_f E_f / 2 \tag{14}$$

$$E_{ls} = k_{es}k_v \rho_{st} E_s / 2 \tag{15}$$

The stress–strain curve in Eq. (13) can be generated by incrementally increasing ε_c in Eq. (13c) and then calculating f_c from Eq. (13a). Note that when $E_{lf} = E_{ls} = 0.0$, f_c calculated using Eq. (11) (or f_c calculated using Eq. (13) is equal to f'_c and $\varepsilon_{co} = \varepsilon_o = 0.002$, and hence the stress–strain curve in the first stage is reduced to that for unconfined concrete.

For unconfined concrete or for the concrete cover of sections confined only internally with ordinary steel and for the purpose of validating the proposed model by comparing with experimental data as illustrated in the next section, the stress–strain relationship in the descending branch of the unconfined stress–strain response is assumed to follow the equation proposed by Scott et al. [16]:

$$f_c = f'_c[1 - Z(\varepsilon_c - \varepsilon_o)] \geqslant 0.2f'_c \quad \text{for } \varepsilon_c \geqslant \varepsilon_o \tag{16}$$

where

$$Z = \frac{0.5}{\frac{3 + 0.29f'_c}{145f'_c - 1000} - 0.002} \tag{17}$$

4. Comparison of analytical predictions with experimental data

The accuracy of the proposed model for circular sections was verified by comparing the analytical results with the test data of Toutanji [8], Nanni et al. [18], Miyauchi et al. [19] and Teng and Lam [15]. Typical comparisons are shown in Fig. 4. The results in Fig. 4 clearly show remarkable agreement between the analytical predictions and the experimental results.

In order to verify the accuracy of the stress–strain model for rectangular column sections, the analytical predictions were compared with the test results obtained recently by Hantouche and Harajli [20], Cole and Belarbi [21], and Tan [5].

In the experiment of Hantouche and Harajli [20], short FRP confined columns with rectangular sections were tested under monotonically increasing axial load to failure. All column specimens were 300 mm long. The test variables included the aspect ratios of the section, the area of FRP reinforcement and the area of internal steel reinforcement. Three aspect ratios of 1.0, 1.7 and 2.3 and three different areas of FRP reinforcement were investigated. The FRP consisted of carbon sheets having a design thickness of
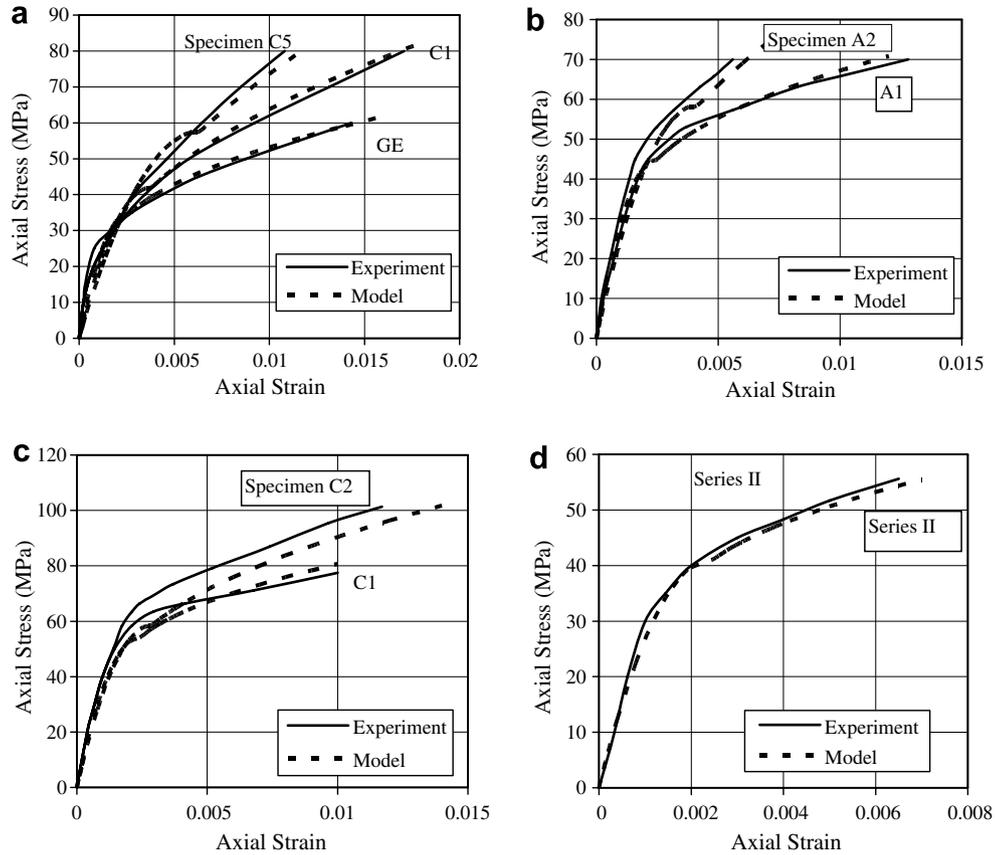
Fig. 4. Comparison of model prediction with experimental results for circular columns (from Hantouche and Harajli [20]): (a) Toutanji [8], (b) Nanni et al. [18], (c) Miyauchi et al. [19], (d) Teng and Lam [15].

0.13 mm per layer, modulus of elasticity of 230,000 MPa, and tensile strength and strain at break of fibers of 3500 MPa and 1.5%, respectively. The corners radius for FRP application was 15 mm for all specimens. The longitudinal steel in the reinforced specimens consisted of 4 ∅ 8 mm – Grade 60 steel bars places at the corners. A summary of input variables for representative specimens is provided in Table 1. Results of comparisons between the analytical predictions and the experimental data are shown in Fig. 5.

In the experiment by Cole and Belarbi [21] rectangular columns were tested to failure in compression. The main variables included the type of fibers, the thickness of FRP jackets, the aspect ratio of the cross section and the radii of the section corners. Only the square columns, for which the full axial force versus strain response were reported, were considered in the comparison. The specimens compared included specimen 1CFRP-Rect1/1, confined with one layer of carbon fiber polymer sheets, and specimens 1GFRP-Rect1/1, 2GFRP, 3GFRP confined with one, two or three layers of glass fiber polymer sheets, respectively. The modulus of elasticity E_f for the carbon fiber sheets is equal to 228 GPa, and that for the glass fiber sheets is equal 72.4 GPa. The design thickness is equal to 0.17 mm and 0.35 mm for the carbon and glass FRP sheets, respectively. All columns have a rectangular cross section

Table 1
Summary of test parameters [20]

Column Specimen	Column dimension $b \times h$ (mm^2)	Aspect ratio	Long. steel	Lateral[a] steel	No. of Carbon FRP layers[b]	Comp. strength, f_c' (MPa)
C1	132 × 132	1.00	–	–	–	18.3
C1FP1	132 × 132	1.00	–	–	1 layer	18.3
C1FP3	132 × 132	1.00	–	–	3 layers	18.3
C1SFP2	132 × 132	1.00	4 ∅ 8 mm	∅6 mm	2 layers	15.2
C1SFP3	132 × 132	1.00	4 ∅ 8 mm	∅6 mm	3 layers	15.2
C2FP2	102 × 176	1.73	–	–	2 layers	18.3
C2SFP1	102 × 176	1.73	4 ∅ 8 mm	∅6 mm	1 layer	15.2
C3FP2	79 × 214	2.71	–	–	2 layers	18.3
C3FP3	79 × 214	2.71	–	–	3 layers	18.3

[a] Spacing = 100 mm.
[b] Thickness per one layer = 0.13 mm.

of 323 cm^2, corner radii of 22.5 mm, unconfined concrete compressive strength of 21 MPa, reinforced with four No. 4 Grade 40 longitudinal steel bars and with transverse reinforcement consisting of 6.4 mm smooth dowels, at a spacing of 178 mm. Results showing the predicted normalized axial stress (ratio of axial stress of the confined specimens to the peak axial strength of the unconfined control specimen) versus strain response in comparison with the test results are shown in Fig. 6.
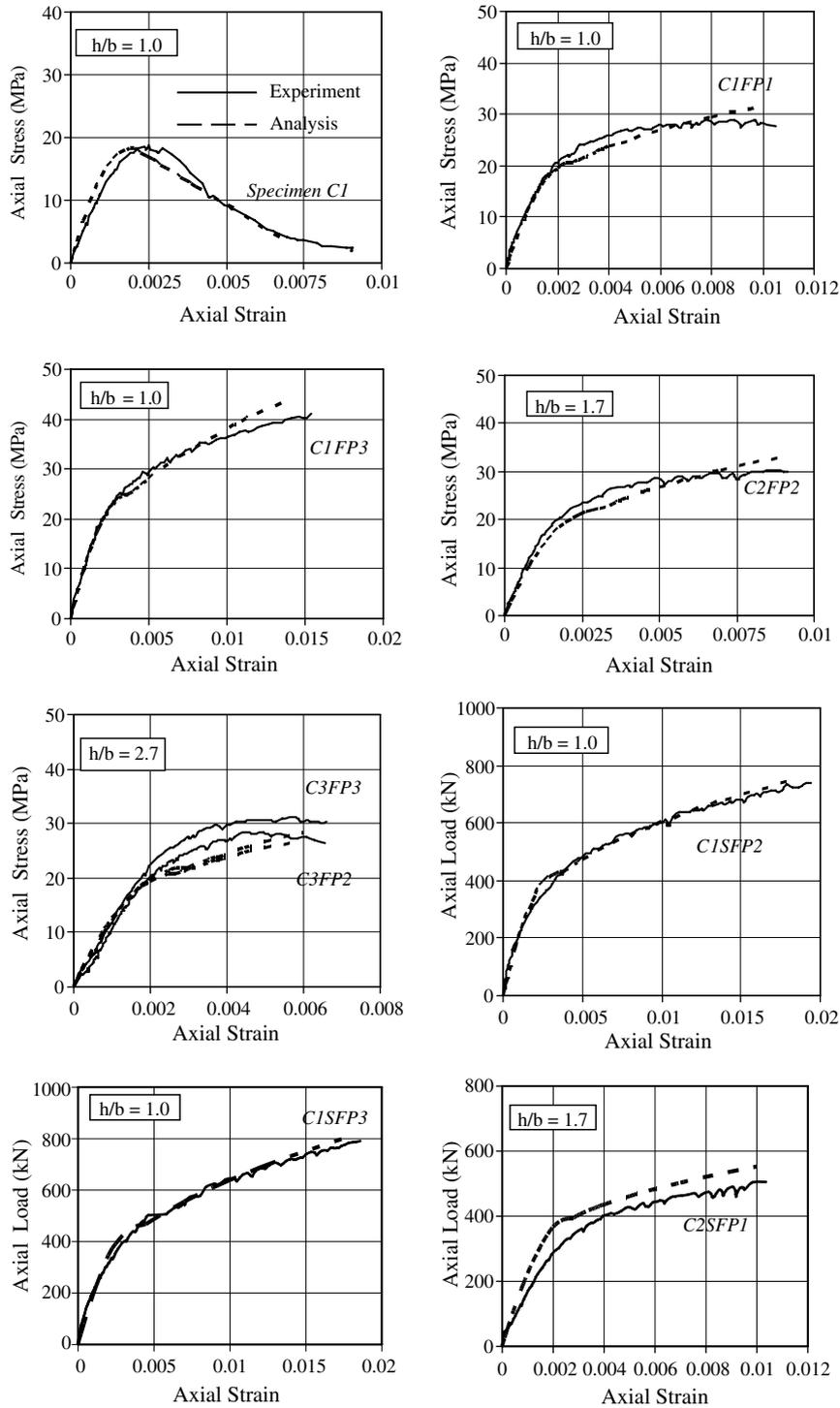
Fig. 5. Comparison of analytical predictions with the experimental results of rectangular columns of Hantouche and Harajli [20].

In the test program of Tan [5], short columns having a 420 × 115 mm section (aspect ratio of 3.7) were tested under axial compression. All columns measured 1.5 m or 1.2 m in height. The internal longitudinal reinforcement consisted of 8 T13 mm bars (total area of 1062 mm²) and the transverse reinforcement consisted of 6 mm diameter hoops spaced at 100 mm in the middle 600 mm length of the columns and 60 mm at the column ends. All columns

were rounded at the corner for FRP application with a radius r of 30 mm. Carbon and/or glass FRP was applied along the transverse direction, as well as the longitudinal direction in different configurations. A summary of the input data for the specimens compared is provided in Table 2. Results of comparisons between the model predictions and experimental data are given in Fig. 7. In reproducing the experimental results, the axial deformation is calculated
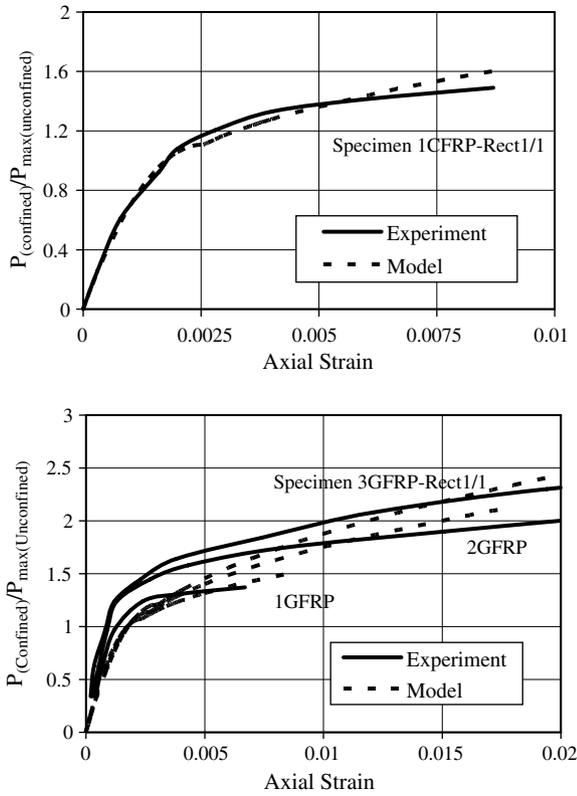
Fig. 6. Comparison of analytical predictions with the test data of Cole and Belarbi [21].

over a gage length of 200 mm used in the experiment and the corresponding axial load P is calculated by taking into account the contribution of the ordinary longitudinal steel and the longitudinal FRP assuming that the contribution of longitudinal fibers to the axial load is effective only up to an axial strain of 0.3% (axial deformation of 0.6 mm) which is the average maximum strain that the longitudinal fibers were reportedly able to sustain.

It is clear from the comparisons presented in Figs. 5–7 that despite the large number of parameters involved for rectangular column sections, in addition to its accuracy in predicting the stress–strain response of circular columns (Fig. 4), the analytical model predicts the stress–strain or axial load–deformation response of rectangular columns having a wide range of section aspect ratios with reason-

able accuracy. Note that the sudden drop in the load resistance at the axial deformation of 0.6 mm in some specimens tested by Tan (Fig. 7) is attributed to the assumption of sudden failure of the longitudinal fibers beyond a strain of 0.3% as indicated earlier.

It is worth mentioning that in an attempt to verify further the accuracy of the proposed model, the analytical predictions were also compared with the test results of Chaallal et al. [3]. Unfortunately, although the size of the specimens and the type and areas of the FRP reinforcement used in the test of Chaallal et al. and those used by Hantouche and Harajli [20] were coincidentially similar, the proposed model predicted significantly larger axial strains for the measured axial stresses and therefore did not compare well with the trend of the stress–strain responses reported by Chaallal et al. as it did for the test results of Hantouche and Harajli (see Fig. 5). It is possible that the method by which the axial strains are measured has a great influence on the shape of the stress–strain response reported by different investigators. For instance, in the experiment by Chaallal et al. [3], the axial strains were reportedly measured locally using strain gauges attached to the specimens at midheight. On the other hand, in the test by Hantouche and Harajli [20], the axial strains were initially measured using transducers attached to the specimens at midheight over a gage length of 200 mm. However, it was observed that beyond an axial strain of 0.002–0.003, as a result of the significant compression cracking that may occur over localized zones outside the gage length, the measured strains, particularly for the FRP confined specimens, were sizably lower than the average strains estimated from the total measured axial deformation of the specimens. Consequently, beyond axial strains of about 0.002–0.003, it was necessary to switch to the average axial strains over the full height of the specimens.

5. Parametric evaluation

The effects of section geometry and unconfined concrete compressive strength on the stress–strain response were evaluated using three different types of sections: circular section, square section and rectangular section. All sections have an area of 2500 cm^2, unconfined concrete strength $f'_c = 25$ MPa, FRP reinforcement $E_f n_f t_f = 90$ kN/mm, and

Table 2
Summary of test data [5]

Specimen[a]	Fiber type		Transverse fibers		Longitudinal fibers		Concrete strength[b] f'_c (MPa)
	Transverse	Longitudinal	E_f (GPa)	$n_f t_f E_f$ (kN/mm)	E_{fa} (GPa)	$A_{fa}E_{fa}$ (kN)	
M00	–	–	–	–	–	–	17.8
M01C	Carbon	–	228	38.0	–	–	20.8
M11C	Carbon	Carbon	228	38.0	228	31.5	15.0
M13G	Glass	Glass	72.4	76.7	72.4	21.2	19.5
M23G	Glass	Glass	72.4	76.7	72.4	27.1	19.2
M12CG	Glass	Carbon	72.4	51.5	228	31.5	20.6

[a] $f_y = 495$ MPa, $E_s = 166$ MPa for long. steel; $f_{yt} = 365$ MPa, $E_s = 211$ MPa for transverse steel.
[b] Cylinder strength f'_c is assumed equal to 80% of the reported cube strength f_{cu}.
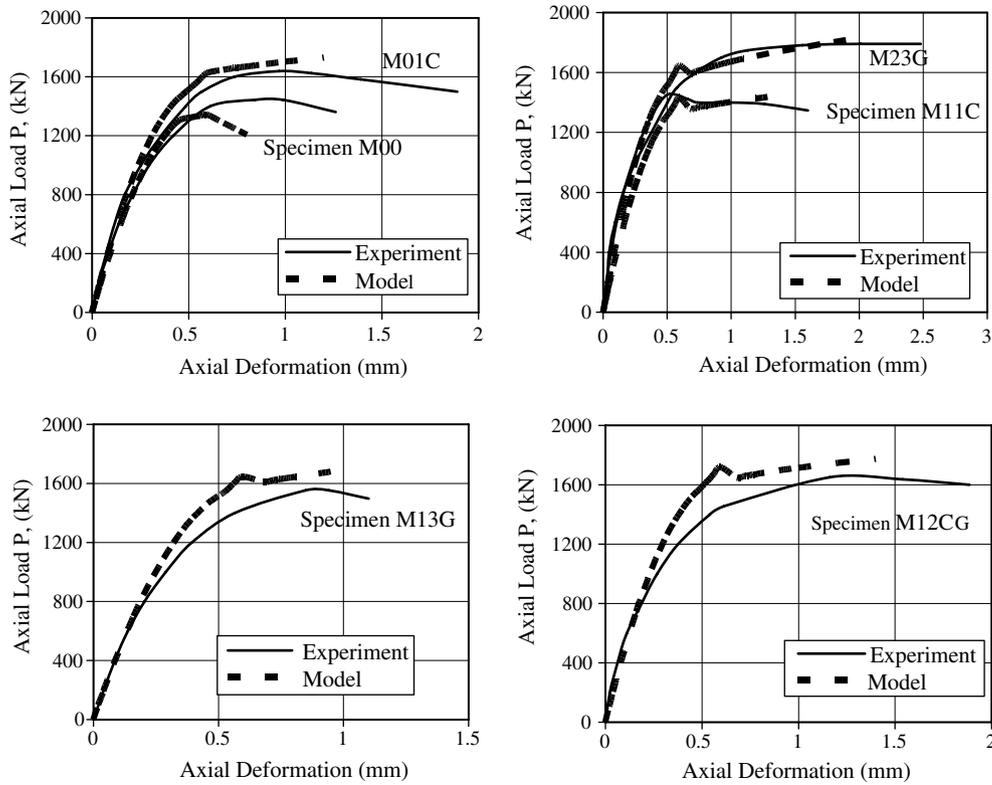
Fig. 7. Comparison of model prediction with the test data of Tan [5].

corner radius (square and rectangular sections) $r = 30$ mm. Typical results are shown in Fig. 8. Fig. 9 shows the effect of corner radius for the same section used in generating the results in Fig. 8, except that h/b was taken equal to 2.0, and Fig. 10 shows the influence of concrete compressive strength on the effectiveness of FRP confinement in increasing the axial stress corresponding to f'_c of 25 MPa (NSC) and 50 MPa (HSC), respectively.

In support of several experimental observations, Fig. 8 clearly predicts that FRP confinement is not as effective in improving the axial strength of rectangular columns as compared to circular ones, and that the corresponding effectiveness decreases sharply as the aspect ratio of the rectangular section increases. Fig. 9 shows that the size of
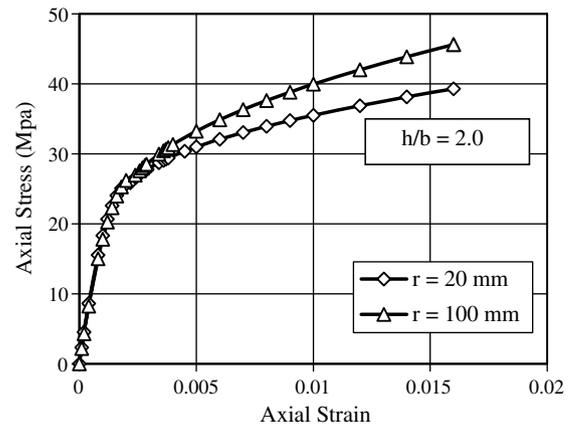

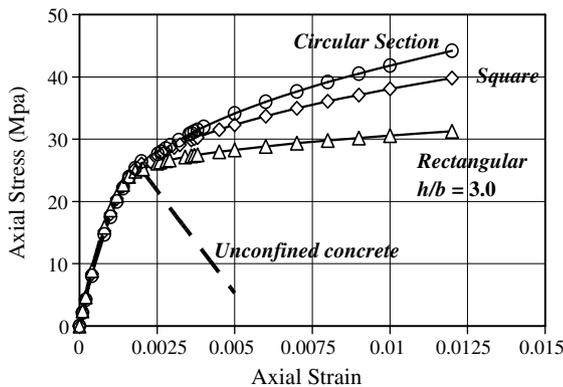Fig. 9. Effect of corner radius on the predicted stress–strain response.

the corner radius has a sizable effect on the stress–strain response of FRP confined concrete. Increasing the corner radius increases the effectively confined concrete area and therefore improves the confinement effectiveness of the FRP. Also, Fig. 10 shows that the effectiveness of FRP confinement in increasing the axial strength decreases with increase in f'_c, which is in agreement with the experimental observation reported by Chaallal et al. [3] for rectangular column sections, and more recently by Mandal et al. [22] for small-scale circular column specimens.

It should be indicated that the stress–strain response of both confined or unconfined concrete is influenced by the
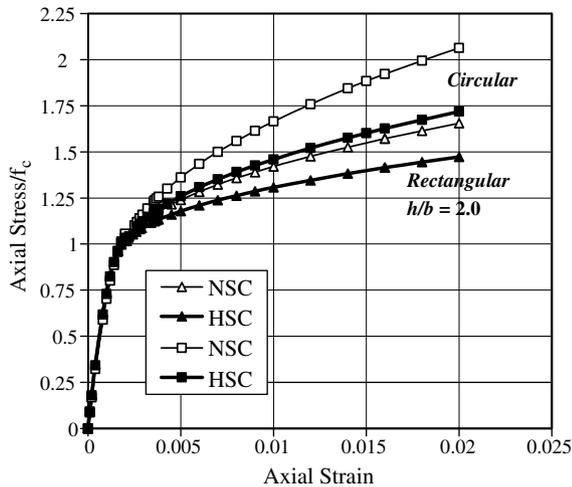

Fig. 8. Effect of section type on the predicted stress–strain response.

Fig. 10. Effect of f'_c on FRP confinement effectiveness in increasing the axial strength.

rate at which the load is applied. Consequently, the proposed model is only applicable for low strain rates of the type encountered under static load application. Also, the proposed analytical model generates a monotonically increasing stress–strain response until the FRP fractures in tension, followed by a brittle failure and total loss of load resistance. However, for design applications, until more experimental data becomes available to justify larger values, it is recommended to limit the axial concrete strain to a value equal to ε_{cu} calculated using Eq. (5) (in which f_c is calculated from Eq. (6)), corresponding to a maximum lateral strain in the FRP recommended by ACI Committee 440 [1] of $\varepsilon_\ell = 0.004 \leqslant 0.75\varepsilon_{fu}$, where ε_{fu} is the fracture strain of the FRP.

6. Conclusions

A general, consistent, and computationally efficient mathematical model is developed to generate the stress–strain (f_c–ε_c) relationship of concrete confined with FRP sheets. The model integrates available confinement models for FRP confined concrete and concrete confined with internal steel and accounts for almost all the parameters that are known to influence the axial strength and stress–strain response of FRP confined axial members. These include type of column section (circular, rectangular), aspect ratio of rectangular section, corner radius prepared in rectangular sections for FRP application, area and properties of the FRP material, and volumetric ratio and arrangement of internal transverse steel ties.

The developed model reproduced accurately experimentally measured stress–strain or load–deformation response of both circular and rectangular column sections. Consistent with the trend of available experimental data, the proposed model predicts that FRP confinement is not as effective in increasing the axial strength of rectangular columns as compared to circular columns and that the corresponding increase in axial strength diminishes sharply

with increase in the aspect ratio of rectangular sections. Also, in support of recent experimental observation, the model predicts that the effectiveness of FRP confinement in increasing the axial strength decreases as the unconfined concrete compressive strength increases.

The proposed stress–strain model can be used very effectively for evaluating the axial load capacity of FRP confined columns and for conducting analytical studies of the response of FRP confined concrete under different types of load application.

Acknowledgements

References

[1] ACI Committee 440. Guide for the design and construction of externally bonded FRP systems for strengthening concrete structures. ACI 440.2R-02, American Concrete Institute, Detroit, MI, 2002.

[2] Chaallal O, Shahawy M. Performance of fiber-reinforced polymer-wrapped reinforced concrete column under combined axial–flexural loading. ACI Struct J 2002;97(4):659–68.

[3] Chaallal O, Shahawy M, Hassan M. Performance of axially loaded short rectangular columns strengthened with carbon fiber-reinforced polymer wrapping. J Compos Const, ASCE 2003;7(3):200–8.

[4] Mander JB, Priestly MJN, Park R. Theoretical stress–strain model for confined concrete. J Struct Engrg, ASCE 1988;114(8):1804–26.

[5] Tan KH. Strength enhancement of rectangular reinforced concrete columns using fiber-reinforced polymer. J Compos Const, ASCE 2002;6(3):175–83.

[6] Saadatmanesh H, Ehsani MR, Li MW. Strength and ductility of concrete columns externally confined with fiber composite straps. ACI Struct J 1994;94(1):434–47.

[7] Mirmiran A, Shahawy M. Behavior of concrete columns confined by fiber composites. J Struct Engrg, ASCE 1997;123(5):583–90.

[8] Toutanji HA. Stress–strain characteristics of concrete column externally confined with advanced fiber composite sheets. ACI Mater J 1999;96(3):397–404.

[9] Harajli MH. Behavior of gravity load-designed rectangular concrete columns confined with FRP sheets. J Compos Const, ASCE 2003;9(1):4–14.

[10] Richart FE, Brandtzaeg A, Brown RL. A study of the failure of concrete under combined compressive stresses. Bulletin 185, University of Illinois Engineering Experimental Station, Champaign, Ill, 1928.

[11] Richart FE, Brandtzaeg A, Brown RL. The failure of plain and spirally reinforced concrete in compression. Bulletin 190, University of Illinois Engineering Experimental Station, Champaign, Ill, 1929.

[12] Elwi AA, Murray DW. A 3D hypoelastic concrete constitutive relationship. J Engrg Mech, ASCE 1979;105(4):623–41.

[13] Lam L, Teng JG. Strength models for fiber-reinforced plastic-confined concrete. J Struct Engrg, ASCE 2002;128(5):612–23.

[14] Teng JG, Lam L. Behavior and modeling of fiber reinforced polymer-confined concrete. J Struct Engrg, ASCE 2004;130(11):1713–23.

[15] Teng JG, Lam L. Compressive behavior of carbon fiber reinforced polymer-confined concrete in elliptical columns. J Struct Engrg, ASCE 2002;128(12):1535–43.

[16] Scott BD, Park R, Priestly MJN. Stress–strain behavior of concrete confined by overlapping hoops at low and high strain rates. ACI J 1982;79(1):13–27.

[17] Sheikh SA, Uzumeri SM. Strength and ductility of tied concrete columns. J Struct Division, ASCE 1980;106(5):1079–102.

[18] Nanni A, Norris MS, Bradford NM. Lateral confinement of concrete using FRP reinforcement. Fiber Reinforced Plastic Reinforcement for Concrete Structures, SP-138, ACI, Farmington Hills, Mich. Berlin, 1994. p. 193–209.

[19] Miyauchi K, Nishibayashi S, Inoue S. Estimation of strengthening effects with carbon fiber sheet for concrete column. Non-metallic (FRP) reinforcement for concrete structures. In: Proceedings of the 3rd international RILEM symposium, vol. 1, 1997. p. 217–24.

[20] Hantouche E, Harajli MH. Axial Strength of FRP Confined Rectangular Column Sections. Ms Thesis submitted by the first author in the Department of Civil and Environmental Engineering, American University of Beirut, Beirut-Lebanon, 2005.

[21] Cole C, Belarbi A. Confinement characteristics of rectangular FRP-jacketed columns. In: Proceedings of the 5th international conference on fiber-reinforced plastics for reinforced concrete structures, Cambridge, UK, 16–18 July 2001. p. 823–32.

[22] Mandal S, Hoskin A, Fam A. Influence of concrete strength on confinement effectiveness of fiber-reinforced polymer circular jackets. ACI Struct J 2005;102(3):383–92.